Article

The Relationship of PM Variation to Visibility and Mixing Layer Height under Haze/Fog Condition in Multi-Cities of Northeast China

Hujia Zhao [1], Huizheng Che [2,*], Yajun Ma [1], Yangfeng Wang [1], Hongbin Yang [1], Yuche Liu [1], Yaqiang Wang [2], Hong Wang [2] and Xiaoye Zhang [2]

[1] Institute of Atmospheric Environment, China Meteorological Administration, Shenyang 110016, China
[2] Key Laboratory for Atmospheric Chemistry, Institute of Atmospheric Composition, Chinese Academy of Meteorological Sciences, CMA, Beijing 100081, China
* Correspondence: chehz@camscma.cn; Tel.: +86-10-58993116

Abstract: The variations of visibility, PM mass concentration and mixing layer height (MLH) at four major urban-industry regions (Shenyang, Anshan, Benxi and Fushun) in multi-cities of central Liaoning over northeast China were evaluated from 2009-2012 to characterize the dynamics effect on air pollution. The annual mean visibilities were about 13.7±7.8km, 13.5±6.5km, 12.8±6.1km and 11.5±6.8km in Shenyang, Anshan, Benxi and Fushun, respectively. The pollution load (PM×MLH) shown a weaker vertical diffusion in Anshan with a higher PM concentration in the near-surface. High concentrations of fine mode particles may be partially attributed to the biomass burning emissions from September in Liaoning Province and surrounding regions in Northeast China as well as the coal burning during the heating period with lower MLH in winter. The increasing wind speed has a similar change as the increasing of mixing layer height to make the effect on the aerosol vertical diffusion. The visibility on the non haze-fog days was about 2.5-3.0 times higher than that on hazy and fog days. The fine particle concentrations of PM2.5 and PM1.0 on the haze and fog days were ~1.8-1.9 times and ~1.5 times higher than that on no hazy-fog days. The MLH during fog pollution showed more declining trend than haze pollution compared with non haze-fog days. The results of this study could provide the useful information to better recognize the effects of vertical pollutants diffusion on air quality in the multi-cities of central Liaoning over Northeast China.

Keywords: Visibility; PM; MLH; multi-cities; Northeast China

1. Introduction

The degradation of visibility has been widely studied to indicate the air quality as one of the key parameters [1-4]. The suspended particles, especially the fine particles in the atmosphere are the primarily factor to impair visibility by scattering and absorbing light [5-8]. The atmospheric particulate matter (PM) pollution could cause a reduction of visibility [9,10] during heavy pollution periods closely related to the meteorological factors [11].

Some studies investigated that visibility degradation has become more seriously in the urban areas than the rural regions because of the rapid urbanization corresponding with increase traffic and higher energy consumption [12-14]. The high aerosol loading from anthropogenic in the urban area contributed to the worse visibility [15] and could influence on local and regional air quality [16-18]. In addition, the atmospheric mixing layer height (MLH) is one of the important meteorological parameter to affect the vertical dispersion of air pollutants and has been studied word widely [19-25].

In China, the certain studies about mixing layer height (MLH) and its implications for air pollution are more focused on the metropolis regions [26-30]. Due to the economic growth and urban expansion, the degradation of visibility has become a new direction for environmental research in

most urban areas of China [31-34]. Zhang et al. [35] and Zhang et al. [36] pointed out that the fine particles could be the principal pollutant that cause the worse visibility in most urban areas in China. The coal combustion and vehicle exhaust could be the primary atmospheric pollution sources to cause visibility degradation in China [37]. Furthermore, four urban regions with serious visibility degradation problem have been divided in China including the Beijing-Tianjin-Hebei Megalopolis (BTH), Pearl River Delta (PRD), Yangtze River Delta (YRD), and Sichuan Basin [38-41]. In particular, these urban areas have also been revealed as the main haze regions in China [42-47]. Therefore, the urban agglomerations will play a more important role in the research on atmospheric changes from the urban scale to the regional scale in China [48, 49].

However, there are few studies focused on visibility degradation, PM concentration and MLH variation for long duration in the urban areas over Northeast China, especially in the "multi-cities" [50]. The multi-cities of central Liaoning (40°00′～42°29′N, 122°10′～125°29′E) is one of the main development base characteristics as heavy industry in China and also one of the few urban concentration area in Northeast Asia. The unique geographical environment and economic structure in the multi-cities of central Liaoning produced many environmental problems, especially the atmospheric visibility problems [51-54]. In this study, we have chosen Shenyang, Anshan, Benxi and Fushun as the representative sites in the multi-cities of central Liaoning (Figure 1) which could feature the visibility ranges and particulate pollution under regional boundary layer dynamics on the typical "multi-city" areas.

Figure 1. Geographic location of multi-cities in central Liaoning over Northeast China.

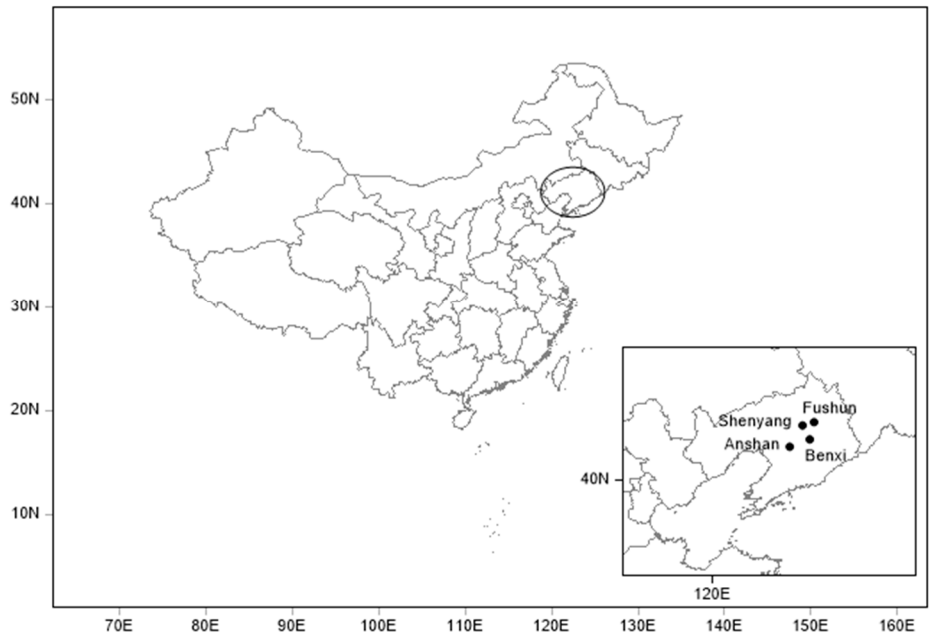

This particle characterized a long-term record of daily visibility, PM mass concentrations data (PM10, PM2.5 and PM1.0) and mixing layer height (MLH) over a period nearly four years from June 2009 to December 2012 in the multi-cities of central Liaoning over Northeast China. The potential relationship between visibility, PM and MLH were also investigated along with the relative humidity (RH), wind speed and direction, respectively. The primary objectives of this paper are aim to (1) present the characteristics of long term observation of visibility, PM concentration and mixing layer height in theses multi-cities in Central Liaoning over Northeast China; (2) better understand the effect of mixing layer height (MLH) on air pollution correlated with meteorological elements in the multi-cities of Central Liaoning. This research indicated the regional air quality on the typical "multi-cities"

in Northeast China which is helpful to provides information for the strategies of visibility improving and particulate matter reduction in other Chinese metropolitan.

2. Sites, Instrument and Data

In this paper, four sites in the multi-cities of central Liaoning over Northeast China were selected for this study. Shenyang (41.77N, 123.50E, 60.0m) is the capital of Liaoning Province, as well as the political, economic and cultural center in Northeast China which could represent the metropolitan areas. Anshan (41.08N, 123.00E, 23.0m), Benxi (41.32N, 123.78E, 183.0m) and Fushun (41.88N, 123.95E, 80.0m) are other three important sites in central Liaoning Province with different geographical feature which reflect the aerosol characteristics in urban-industrial area in Northeast China. The multi-cities of central Liaoning are the important economic development region in Northeast China which is affected by both industrial emissions and residential activities. The air quality there could be linked to the local industry development as well as the transportation in the nearby regions. Thus, the atmospheric pollution problem shows the mutual influence and mutual transformation of the multi-cities in central Liaoning with an obvious characteristic of regional pollution in large area.

A FD12 visibility automatic observation instrument and a GRIMM180 particle instrument were used to obtain visibility and PM (PM10, PM2.5 and PM1.0) mass concentrations at the four sites since June 2009. The measuring time of FD12 instrument is 15s with anaccuracy of ±10% between 0.01km–10km and ±20% between 10km–50km, and the measuring range is 10–50,000m. The measuring time of GRIMM180 is 1–60min which performance with an accuracy of ±2% and the measuring range is 1–1,500μg/m3. The daily and monthly values of visibility and PM mass concentration were calculated by the 10-min average visibility measurements and 5-min average mass concentration measurements using statistical analysis to characterize their properties. The observation days of visibility and PM (PM10, PM2.5 and PM1.0) at Shenyang, Anshan, Benxi and Fushun were 1232, 1295, 1044, 426 and 1220, 1272, 1188, 1174, respectively. The fewer observation data of visibility in Fushun is not as good as other three sites could be due to the instrument problem. In addition, the daily meteorological data including relative humidity (RH), wind speed and direction were also collected from June 2009 to December 2012. The daily mixing layer height (MLH) were obtained by the average of hourly MLH which was calculated based on total cloud cover, low cloud cover and wind speed according to the Technical Guidelines for Environmental Impact Assessment of China [55].

3. Results and Discussion

3.1. Annual Average of Visibility, PM Mass Concentration and MLH in the Four Sites

Table 1 listed the multi annual values of visibility, PM mass concentration (PM10, PM2.5 and PM1.0) and mixing layer height (MLH) from June 2009 to December 2012 in multi-cities of central Liaoning.

Table 1. Annual averages of visibility, PM mass concentration and the mixing layer height in the multi-cities of central Liaoning

Sites	Visibility/(km)	PM_{10}/(μg/m³)	$PM_{2.5}$/ (μg/m³)	$PM_{1.0}$/ (μg/m³)	PM_{10}×MLH(mg/m²)	$PM_{2.5}$×MLH(mg/m²)	$PM_{1.0}$×MLH(mg/m²)	MLH/(m)
Shenyang	13.7±7.8	69.8±37.6	49.1±27.3	43.1±26.2	35.5±21.3	24.5±14.0	21.3±12.9	535.8±207.0
Anshan	13.5±6.5	102.0±63.3	58.8±36.3	49.2±31.8	51.7±40.5	28.1±17.2	23.3±14.7	517.4±212.7
Benxi	12.8±6.1	81.8±45.3	56.4±33.1	47.5±29.2	35.8±23.5	23.8±13.2	19.8±11.5	457.6±195.9
Fushun	11.5±6.8	71.8±55.2	43.9±28.9	37.2±25.5	33.7±30.9	19.7±12.7	16.5±10.4	484.1±191.0

The multi annual visibility was about 13.7±7.8km, 13.5±6.5km, 12.8±6.1km and 11.5±6.8km during the 4-year period in Shenyang, Anshan, Benxi and Fushun, respectively. The multi annual mean visibility in these four sites were much lower than the value of national averaged level of visibility (~26.00km) according to Che et al. [49], which suggests the poor atmospheric quality over the multi-cities of central Liaoning in Northeast China. The multi annual PM2.5 mass concentrations were about 49.1±27.3μg/m3, 58.8±36.3μg/m3, 56.4±33.1μg/m3 and 43.9±28.9μg/m3 in Shenyang, Anshan, Benxi and Fushun, respectively, which all exceeded the annual limit of China's national ambient air quality standards (35μg/m3) (GB3095-2012:http://kjs.mep.gov.cn/hjbhbz/bzwb/dqhjbh/dqhjzlbz/201203/t20120302_224165.htm). In addition, the annual concentration of PM10 in Anshan was 102.0±63.3μg/m3 which was almost 1.2-1.4 times larger than the other three sites and the results indicate an obvious local pollution of coarse mode particles in this urban-industrial area. The multi annual mixing layer height (MLH) was about 535.8±207.0m, 517.4±212.7m, 457.6±195.9m and 484.1±191.0m in Shenyang, Anshan, Benxi and Fushun, respectively. The MLH is a parameter that indicates the pollution dilution effect which means a better air quality conditions in Shenyang with higher mixing layer than the other three sites.

Furthermore, the pollution load (PM×MLH) has been considered in this study in order to exclude the influence of MLH on PM mass concentration according to He et al. [56] and Li et al. [57]. According to the list of Table 1, the near-surface particulate matter concentration in Anshan was mainly highest among the four sites, while the pollution load (PM × MLH) in the mixing layer was not that extremely higher. However, the particulate matter concentration in the near-surface is lower in Shenyang, while the pollution loads (PM × MLH) was corresponding higher in the four sites. These results show that the weaker vertical diffusion maybe caused the high PM concentration in the near-surface in Anshan. While in Shenyang, the highest pollution load (PM × MLH) may due to the contribution of pollutants transportation and the local emission sources [52].

3.2. Monthly and Seasonal Variations of Visibility，MLH and Meteorological Elements in the Four Sites

As seen in Figure 2, the monthly visibility is higher in March and September while lower in July and January in the four multi-cities. The maximum visibility is about 19.1±8.4km occurred in March over Shenyang and the minimum visibility occurred in January over Fushun with an average value about 6.0±3.3km. There is a similar pattern between visibility and MLH. The monthly mean of mixing layer shows a peak value in April (623-726m) and fall to the lower value in August (424-496m). Then the MLH increased to a secondary peak in September (438-519m) and decreased again in January (322-387m). The RH is lower (less than 60%) in March-April-May, while higher in June-July-August (more than 80%). Compared with the higher temperature, the high RH has enhanced the photochemical transformation of secondary aerosols, favors higher concentration of fine mode particles [58]. Monthly mean wind speed is about 2.5m/s in April and reduce to 2.0m/s in August, then increased to the high speed ～3.0m/s in November, then continue reduce to 2.0m/s in January.

The variation of MLH may be related to the seasonal radiation flux during the year to affect visibility by vertical pollutants diffusion as Figure 3 described [59, 60]. The patterns of wind speed reveals that a large number of aerosols have being carried into the atmosphere due to strong winds in spring. The significantly lower wind speeds in summer possibly causing a high PM concentration accumulation, which then reduces visibility. The increasing wind speed in autumn has accelerated the aerosol concentration from biomass burning by regional transportation. The slightly weaker winds in the winter limited the dispersion of pollutants in the cold season.

Figure 2. Monthly variations of (a) visibility, (b) the mixing layer height, (c) Relative Humidity and (d) Wind speed in the multi-cities of central Liaoning

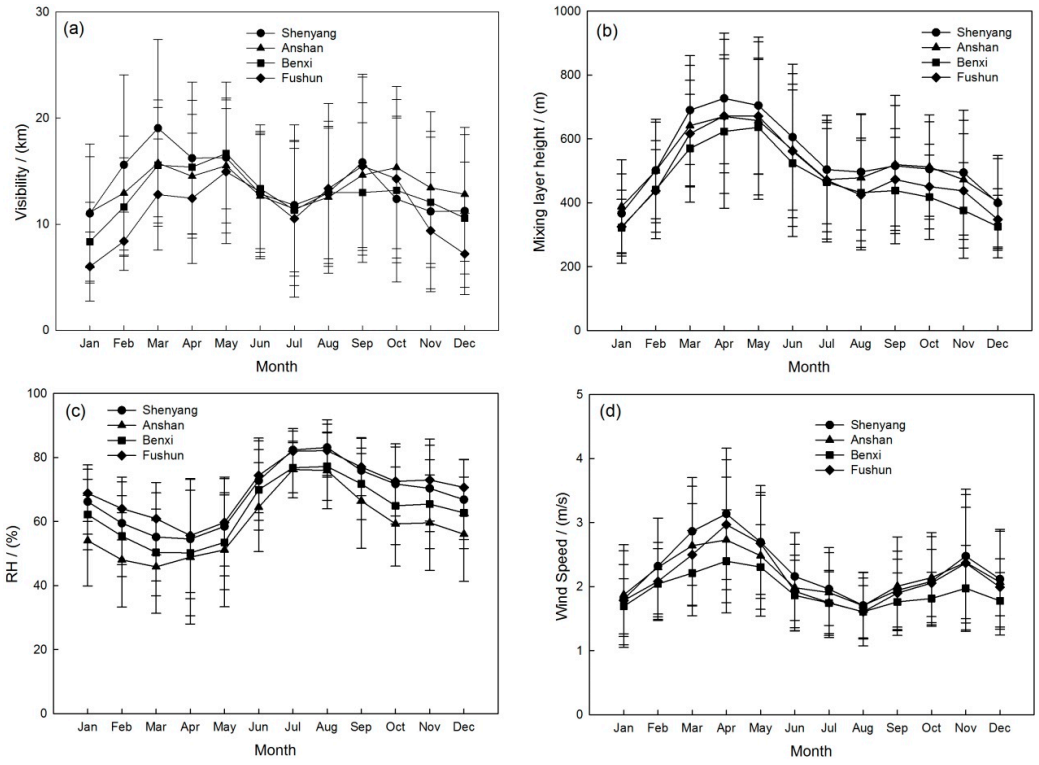

Figure 3. Seasonal variations of (a) visibility, (b) the mixing layer height, (c) Relative Humidity and (d) Wind speed in the multi-cities of central Liaoning

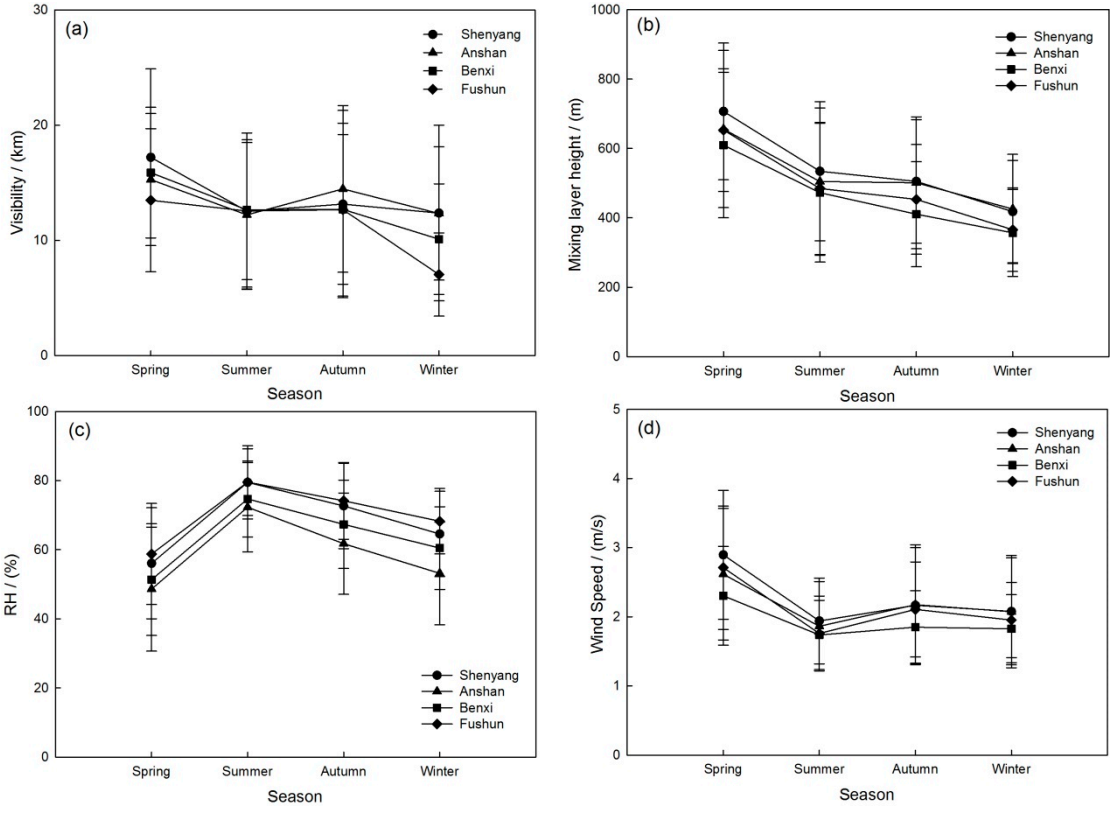

The prevailing winds in different seasons during the observation period over the four sites were also shown in Figure 4. The seasonal wind patterns could contribute to the transportations of pollutants influencing the PM mass concentrations. In spring (March-April-May), the prevailing wind flow is mainly from the south or southwest with a poor atmosphere stability which is easy to form dust weather. In summer, the prevailing wind is mainly from the south or southeast which could provide regional transport of water vapor transmission from southern regions which are easily to form fog weather. Affected by Changbai mountain high pressure, the prevailing winds are mainly from the southeast in the autumn and winter, the cold air fell down from the mountain and make a strong radiative cooling in the ground to formation an inversion layer. This climate mechanism leads to accumulation of contamination in close to the ground.

Figure 4. Seasonal variations of Wind direction in (a) Shenyang, (b) Anshan, (c) Benxi and (d) Fushun in the multi-cities of central Liaoning.

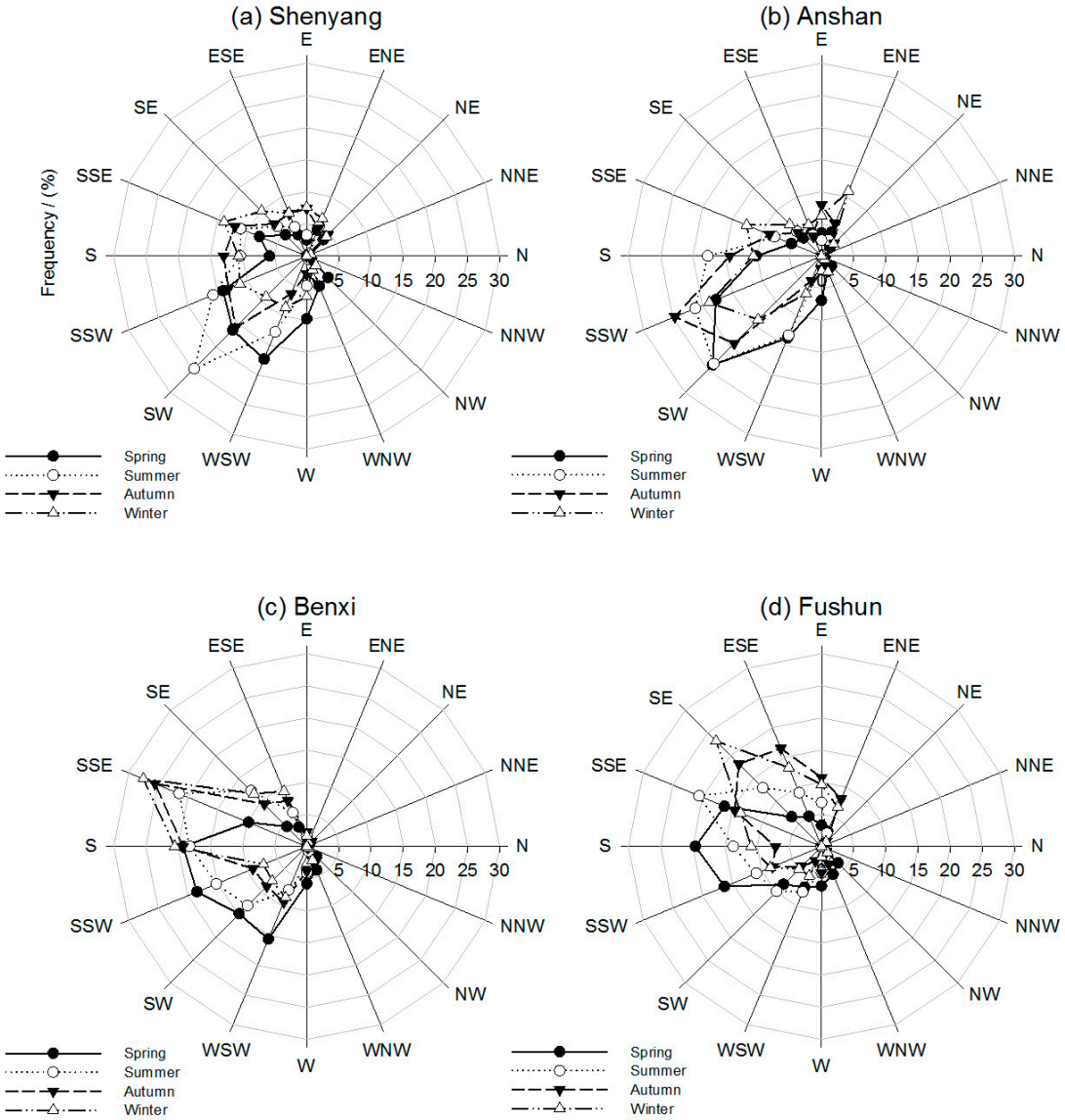

3.3. Monthly Variations of Coarse and Fine mode Particles Mass Concentration in the Four Sites

In this section, a significantly different characteristic between coarse and fine mode particles mass concentration over the four sites were descripted in Figure 5. The concentration of coarse mode particles has an obviously surge in March-April-May which represent the large number of coarse mode aerosol produced by dust storms and wind erosion in the spring results in high aerosol loading

[52]. However, the corresponding visibility in this period was not relatively decreased, which denote that the coarse particle is not the main cause to affect the visibility in the spring time. There were two peaks in the fine mode particles concentration distribution which is usually observed in Jun-July-August and October-November-December-January to the next year. The longer and stronger solar irradiation during summer time can favor the photochemical formation of secondary aerosol particles that lead to the higher fine particle levels in this period [61, 62]. However, the more precipitation could reduce the concentration of the aerosols to a smaller peak value.

Figure 5. Monthly variations of PM mass concentration and PM Ratio in (a) Shenyang, (b) Anshan, (c) Benxi and (d) Fushun in the multi-cities of central Liaoning

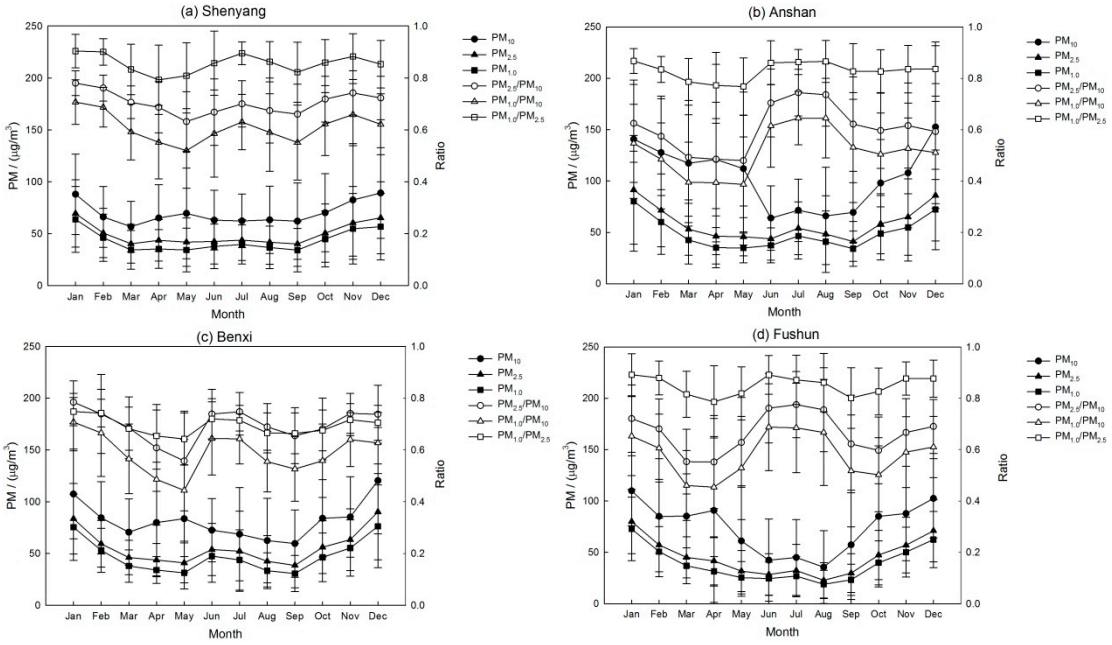

Especially, it is interesting to note that the fine particle concentration has increased somewhat from September to November and has retained a steady level lasted the whole winter even to the January in the next year. High concentrations of fine mode particles may be partially attributed to the biomass burning emissions from September which is the most active month in Liaoning Province and surrounding regions in Northeast China [63, 64]. In addition, the fine mode particles increased in the winter result from a combination of increased emissions from heating sources and low mixing layer height as Figure 2b shown [65, 66]. The residents living heating could be one of the typical pollution in multi-cities leads to the highest BC concentration in winter [67, 68, 48, 49].

Figure 5 also shows that the ratios of PM2.5/PM10 and PM1.0/PM10 grew obviously in summer and winter, while in spring the ratio decreased significantly. The change of PM ratio is slightly in Shenyang while remarkable in the other three sites. The steady higher level of PM ratio in Shenyang highlights the contribution of anthropogenic pollutants due to the soaring urbanization as the capital of Liaoning province. In general, dust events, combustion activities as well as secondary aerosol are the three major sources of PM in the multi-cities of Liaoning province over Northeast China.

3.4. Relationship between Visibility, PM Mass Concentration and MLH with Wind Speed and Direction

The correlation between visibility, coarse and fine mode particles, wind speed and mixing layer height has been established to simple describe the vertical transport of particles in the four sites. Figure 6 indicated that the PM2.5 mass concentration increased exponentially with mixing layer height decreased and the correlation coefficients of the MLH and fine mode particulate were better than the coarse mode particles in Shenyang, Anshan, Benxi and Fuhsun, respectively (Table 2). The correlation between the visibility and MLH was plotted in Figure 7. The correlation coefficients of the visibility and MLH were 0.32, 0.28, 0.42 and 0.40 in Shenyang, Anshan, Benxi and Fuhsun,

respectively which indicates that higher MLH has a good influence on atmospheric visibility (Table 2). Moreover, the relationship between the visibility and MLH under different RH ranges was also considered but the results show that the relationship between the visibility and MLH is not improved as RH increased compared to the studies of Tang et al. [29]. Tang et al. [29] indicated that high RH may be favor of local contribution of humidity related physicochemical processing in heavy pollution which need the vertical transportation of MLH to get better visibility. While in this paper, the RH may do not have the same significant impact on the aerosol physicochemical processing to enhance the correlation between visibility and MLH which need further study.

Table 2. The correlation coefficient between PM mass concentration, visibility, wind speed and mixing layer height in the four sites.

Site	PM_{10} vs. MLH	$PM_{2.5}$ vs. MLH	$PM_{1.0}$ vs. MLH	VIS vs. MLH	Wind Speed vs. MLH
Shenyang	-0.24	-0.31	-0.33	0.32	0.60
Anshan	-0.05	-0.27	-0.30	0.28	0.60
Benxi	-0.20	-0.33	-0.35	0.42	0.60
Fushun	-0.14	-0.33	-0.36	0.40	0.64

Figure 6. Scatter plot of PM2.5 mass concentration and MLH in (a) Shenyang, (b) Anshan, (c) Benxi and (d) Fushun in the multi-cities of central Liaoning.

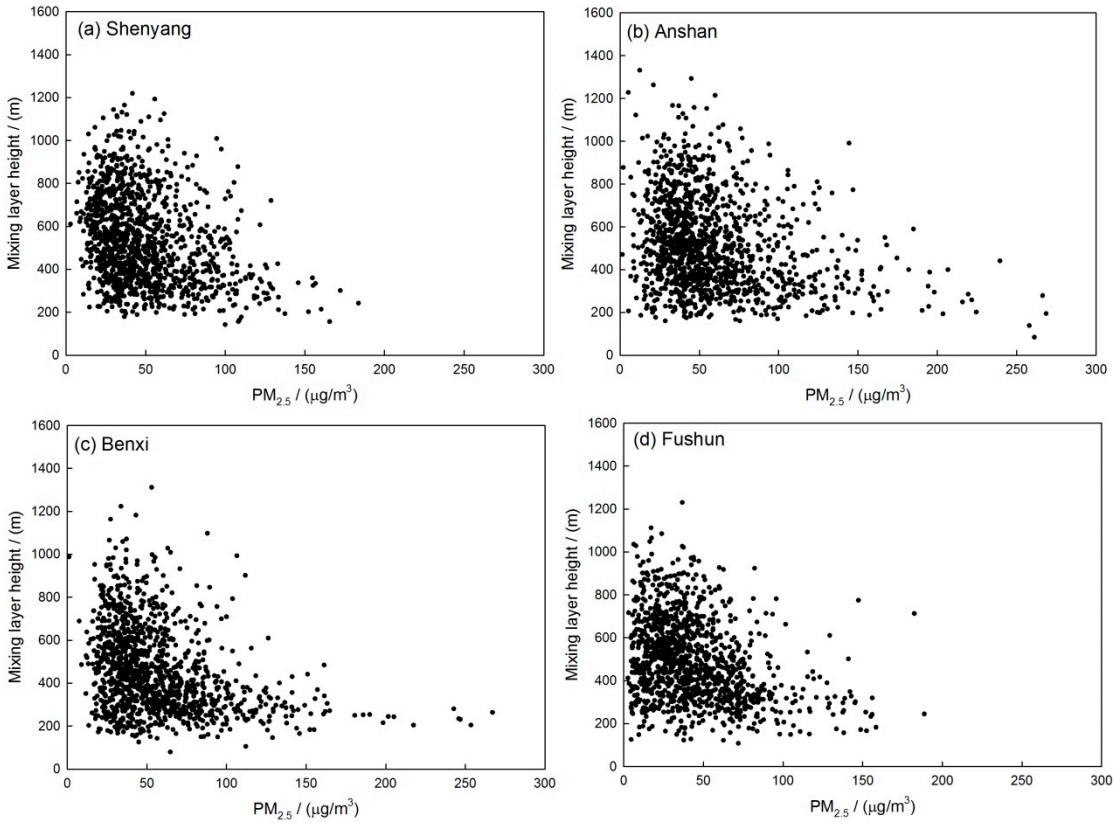

Peer-reviewed version available at Int. J. Environ. Res. Public Health 2017, 14, , 471; doi:10.3390/ijerph14050471

Figure 7. Scatter plot of Visibility and MLH in (a) Shenyang, (b) Anshan, (c) Benxi and (d) Fushun in the multi-cities of central Liaoning

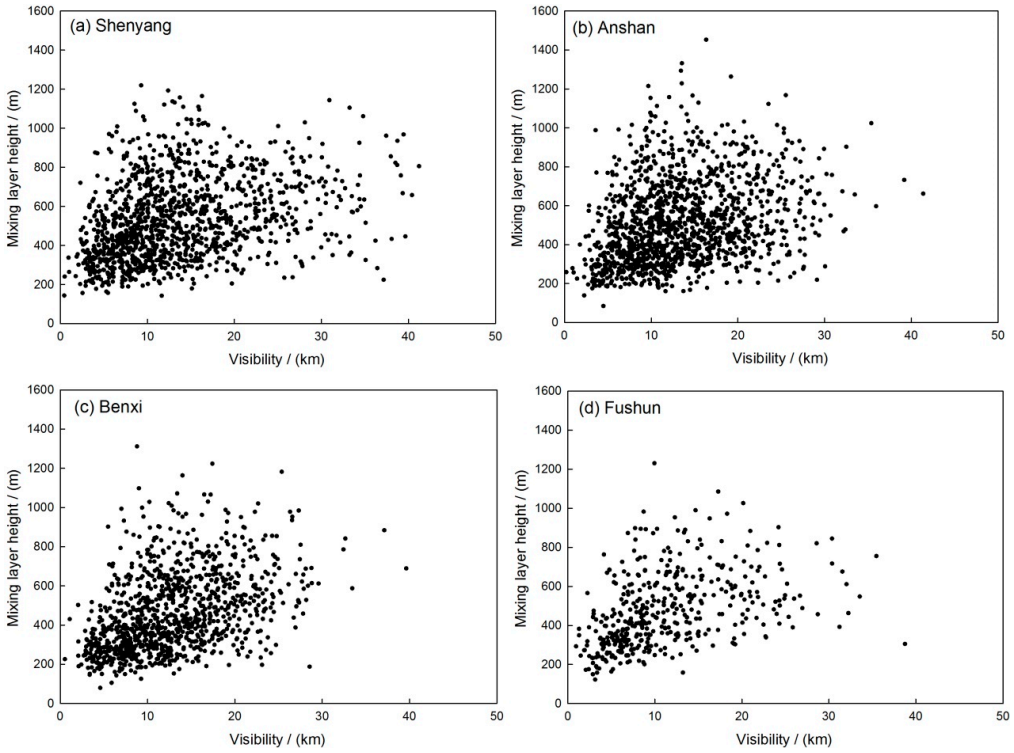

The relationship between MLH and wind speed is illustrated in Figure 8 to present the impact on the vertical and horizontal pollution diffusion. There was a good correlation between MLH and wind speed (~0.60) in these four sites. The increasing wind speed has a similar change as the increasing of mixing layer height which has an effect on the aerosol vertical diffusion.

Figure 8. Scatter plot of Wind Speed and MLH in (a) Shenyang, (b) Anshan, (c) Benxi and (d) Fushun in the multi-cities of central Liaoning

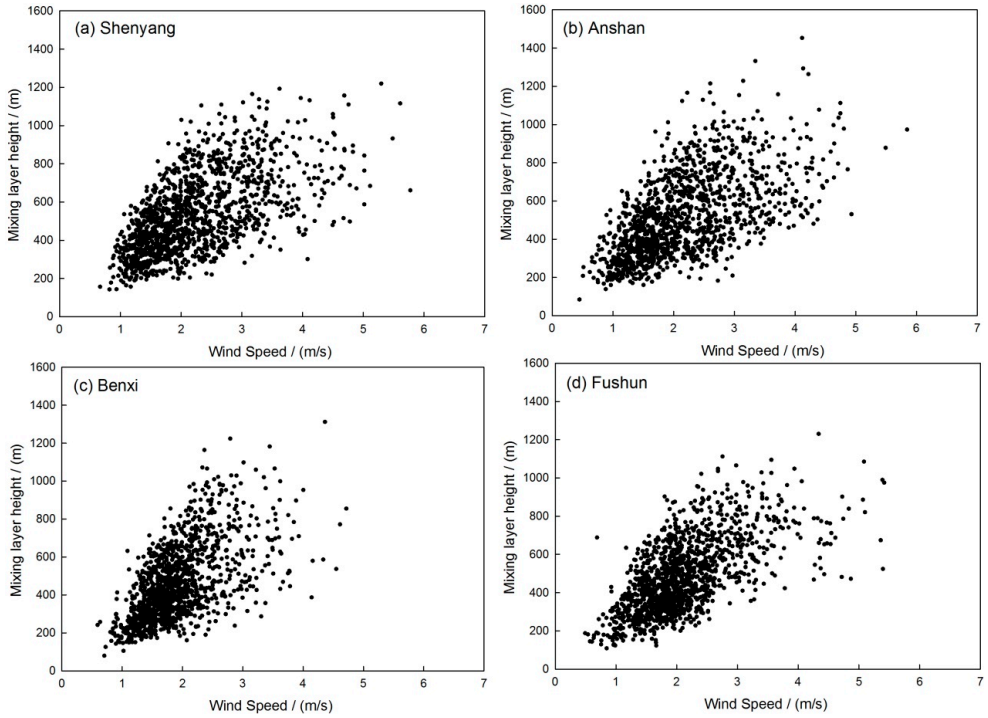

Preprints (www.preprints.org) | NOT PEER-REVIEWED | Posted: 20 March 2017 doi:10.20944/preprints201703.0160.v1

Peer-reviewed version available at Int. J. Environ. Res. Public Health 2017, 14, , 471; doi:10.3390/ijerph14050471

Co-variation between visibility, PM concentration and wind direction in the multi-cities were also shown in Figure 9 to describe the horizontal variation in the air pollution. In Shenyang, the wind flow from the North-West has the larger visibility about 25km compared with the lower level of PM concentration. In Anshan, the wind flow from the North-North-West has the larger visibility about 23km compared with the lower level of PM concentration. Unlikely Shenyang and Anshan, the wind directions in North-East have the larger visibility about 21km compared with the lower PM concentration in Benxi and Fushun. On the contrary, the wind flow from the North-North-East has the higher PM concentration with lower visibility about 10km in Shenyang. In other three sites, the wind flow from the South-West has the largest PM concentration. Therefore, the airflow from North of Liaoning province could carry the clear air to the multi-cities while the airflow from South-West may convey the pollution air from inland China.

Figure 9. The variations of (a) visibility, (b) PM10, (c) PM2.5 and (d) PM1.0 on the different wind direction in the multi-cities of central Liaoning

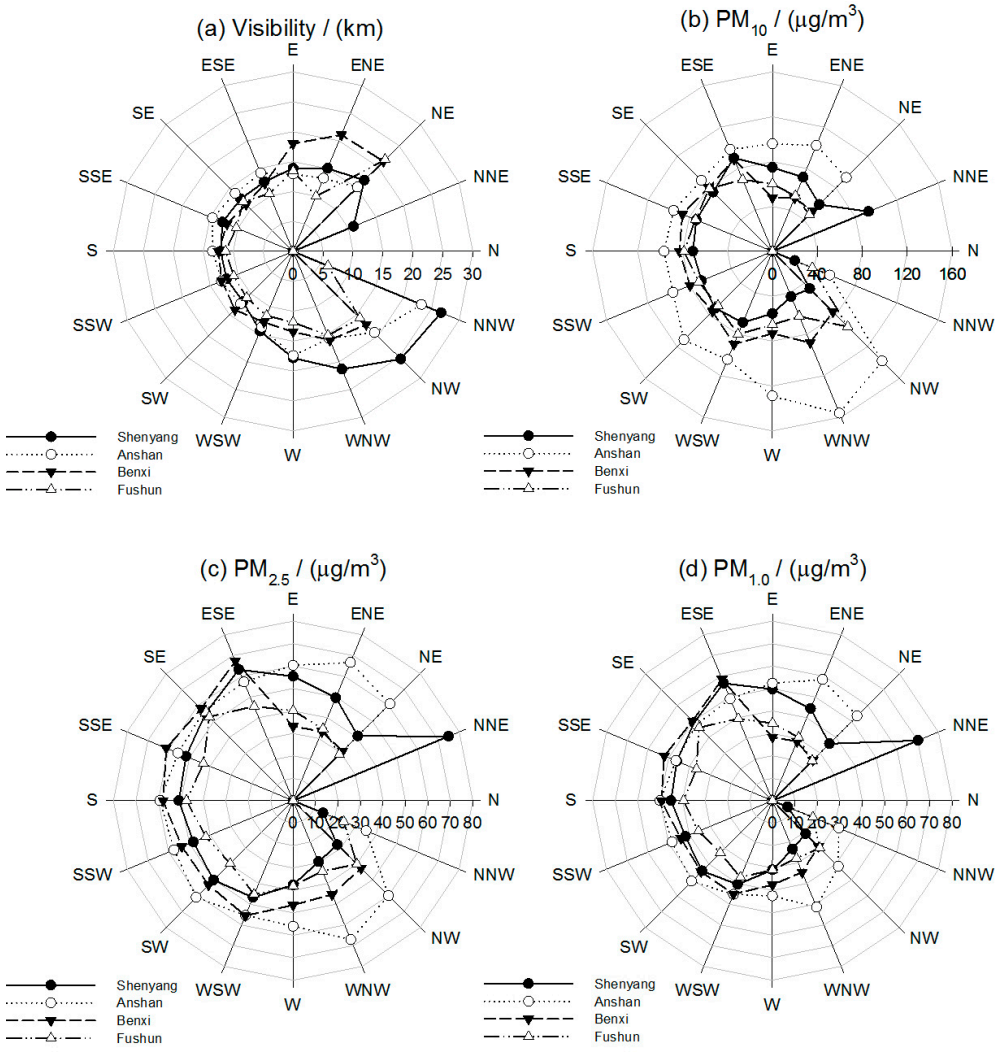

3.5. Variations in Visibility and PM under Horizontal and Vertical Meteorological Elements during Pollution Episodes

The days and distribution of visibility >19km and <10km in multi-cities of central Liaoning was shown in Figure 10 as classified according to Gomez and Smith [69] which has an inverse correlation in contrast to the mixing layer height.

The days of visibility <10km are more occurred from June to January and February in the next year while the days of visibility >19km are more occurred in March-April-May. The distribution of

Preprints (www.preprints.org) | NOT PEER-REVIEWED | Posted: 20 March 2017 doi:10.20944/preprints201703.0160.v1

Peer-reviewed version available at Int. J. Environ. Res. Public Health 2017, 14, , 471; doi:10.3390/ijerph14050471

low visibility between 8.0km and 10.0km has the most frequent accounting for about 28.8%-37.9%. The low visibility ranged in 6.0-8.0km are accounting for 29.9%-33.1% of the total occurrence. The low visibility less than 1km was extremely scarce in the four sites. The good visibility ranged in 19-24km and 24-29km are accounting for 47.4%-69.4% and 27.2%-32.2%, respectively.

Figure 10. The Observation days of (a) visibility<10km and (b) visibility >19km and the distributions of (c) visibility<10km and (d) visibility >19km in the multi-cities of central Liaoning

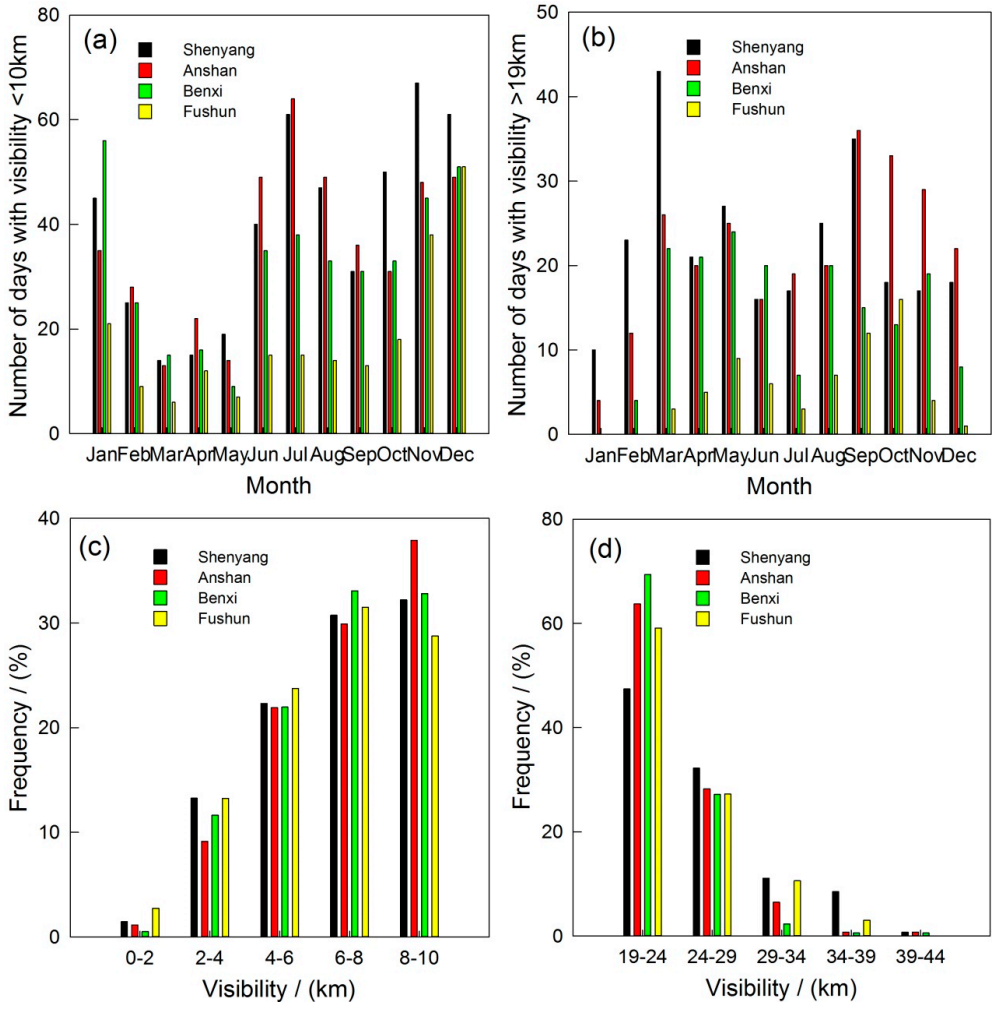

In this study, haze episode is defined as the RH<90% and visibility ≤10km [70]. Non-haze period is the one with RH<90% and visibility>10km. Fog episode is under the conditions of RH≥90% and visibility ≤10km [71].

The variations of visibility, PM mass concentration and MLH under different meteorological conditions during haze, fog, non haze-fog days were shown in Table 3. The visibility during haze and fog episode is about 6.7±2.1km, 7.0±2.1km, 6.9±2.1km, 6.4±2.2km and 6.1±2.6km, 6.3±2.3km, 6.1±1.9km and 6.0±2.9km at Shenyang, Anshan, Benxi and Fushun, respectively. The visibility on the non haze-fog days was about 2.5 and 3.0 times higher than that on hazy and fog days. The PM2.5 and PM1.0 during haze episode were about 70.8±30.1μg/m3, 87.5±44.3μg/m3, 80.0±36.2μg/m3, 64.2±32.3μg/m3 and 64.0±28.7μg/m3, 75.2±38.8μg/m3, 68.7±32.6μg/m3, 55.2±28.9μg/m3 in the four sites, respectively. The PM2.5 and PM1.0 during fog episode were about 53.5±27.8μg/m3, 71.4±52.1μg/m3, 72.5±49.9μg/m3, 51.4±48.2μg/m3 and 48.6±26.2μg/m3, 61.7±40.2μg/m3, 58.6±38.0μg/m3, 44.4±41.0μg/m3 in the four sites, respectively. The fine particle concentrations of PM2.5 and PM1.0 on the haze days were ~1.8-1.9 times higher than that on no hazy-fog days, while on fog days, the concentrations of PM2.5 and PM1.0 were ~1.5 times higher than that on no hazy-fog days.

Table 3. The average visibility, PM mass concentration, PM ratio and meteorological elements during the haze, fog and non haze-fog episode in the multi-cities of central Liaoning

Site	Shenyang			Anshan			Benxi			Fushun		
VIS(km)/ /RH(%)/ WS(m/s)/ MLH (m)	VIS/ RH/ WS/MLH			VIS/ RH/ WS/MLH			VIS/ RH/ WS/MLH			VIS/ RH/ WS/MLH		
Haze	6.7±2.1/74.4±10.3/2.0±0.8/467.7±187.6			7.0±2.1/66.8±13.8/2.0±0.9/449.3±202.5			6.9±2.1/70.5±11.2/1.8±0.6/376.3±171.5			6.4±2.2/73.2±10.0/2.0±0.7/410.1±175.4		
Fog	6.1±2.6/94.1±3.1/1.8±0.6/379.5±174.3			6.3±2.3/94.2±2.6/1.9±0.7/427.0±161.2			6.1±1.9/94.2±2.9/1.4±0.4/285.9±104.8			6.0±2.9/91.2±1.0/1.5±0.4/347.2±117.6		
Non haze-fog	18.1±6.8/63.3±15.0/2.4±0.9/585.5±203.5			16.9±5.3/54.7±16.1/2.3±0.9/555.0±210.0			16.4±4.9/60.4±14.7/2.0±0.6/499.0±193.6			16.9±5.8/68.6±12.8/2.2±0.8/511.0±189.0		
PM /(μg/m^3)	PM_{10}	$PM_{2.5}$	$PM_{1.0}$	PM_{10}	$PM_{2.5}$	$PM_{1.0}$	PM_{10}	$PM_{2.5}$	$PM_{1.0}$	PM_{10}	$PM_{2.5}$	$PM_{1.0}$
Haze	94.7±38.9/70.8±30.1/64.0±28.7			126.9±72.5/87.5±44.3/75.2±38.8			106.5±47.2/80.0±36.2/68.7±32.6			93.2±57.8/64.2±32.3/55.2±28.9		
Fog	82.6±66.2/53.5±27.8/48.6±26.2			85.1±64.0/71.4±52.1/61.7±40.2			100.0±79.2/72.5±49.9/58.6±38.0			81.5±105.1/51.4±48.2/44.4±41.0		
Non haze-fog	57.5±26.4/38.4±17.4/32.6±16.8			92.2±54.8/45.3±19.7/36.9±17.0			71.7±38.2/46.4±24.4/38.5±21.3			68.1±50.6/40.3±25.9/34.1±23.0		

Peer-reviewed version available at Int. J. Environ. Res. Public Health 2017, 14, , 471; doi:10.3390/ijerph14050471

The RH during haze and fog days were 74.4 ± 10.3, 66.8 ± 13.8, 70.5 ± 11.2, 73.2 ± 10.0 and 94.1 ± 3.1, 94.2 ± 2.6, 94.2 ± 2.9, 91.2 ± 1.0 for Shenyang, Anshan, Benxi and Fushun, respectively, which is much higher than the values on non-hazy days. The average wind speed during haze and fog days were 2.0± 0.8m/s, 2.0±0.9m/s, 1.8±0.6m/s, 2.0±0.7m/s and 1.8±0.6m/s, 1.9±0.7m/s, 1.4±0.4m/s, 1.5±0.4m/s for Shenyang, Anshan, Benxi and Fushun, respectively, which was lower compared to non-haze days.

The mixing layer height is an important meteorological factor to analyze the dynamic effects in air pollution. The mixing layer height during haze and fog episode is about 467.7±187.6m, 449.3±202.5m, 376.3±171.5m, 410.1±175.4m and 379.5±174.3m, 427.0±161.2m, 285.9±104.8m and 347.2±117.6m at Shenyang, Anshan, Benxi and Fushun, respectively. The MLH on the non haze-fog days was about 1.2 and 1.5 times higher than that on hazy and fog days. The results noted that compared with non haze-fog days, MLH during fog pollution showed more declining trend than haze pollution which indicate the relatively large impact of dynamic effects on the fog pollution in the multi-cities of central Liaoning. Through the analysis of a fog episode happened on November 29th to December 1st over the multi-cities of central Liaoning in northeast China, the horizontal and vertical meteorological elements has been shown in Figure 11-12. As the thermal/dynamic parameters described, the mixing layer height is lower to nearly 200m compared with the stable weather condition of temperature inversion and small wind speed in the near-surface during the fog pollution by significant visibility deterioration.

Figure 11. The variation of (a) visibility, (b) mixing layer height, (c) RH and (d) wind speed during the fog episode in the multi-cities of central Liaoning

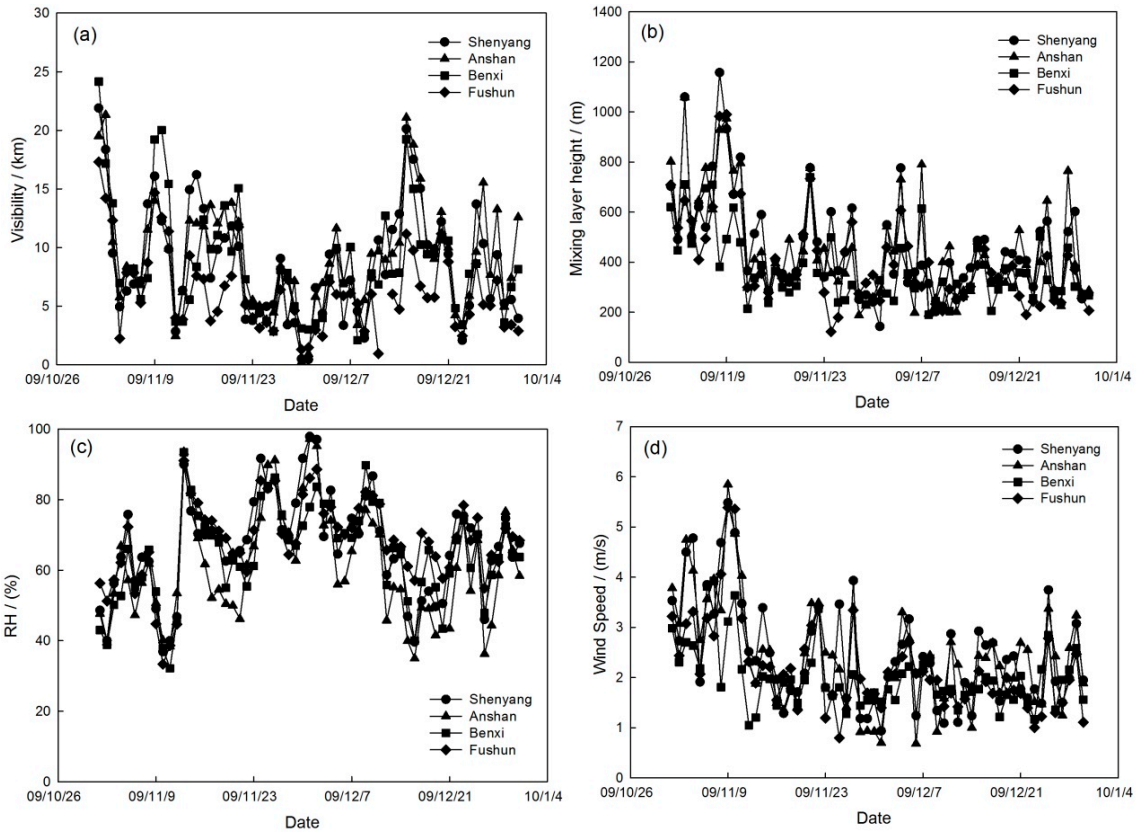

Figure 12. The vertical variation of (a) Temperature and (b) wind speed during the fog episode in the multi-cities of central Liaoning

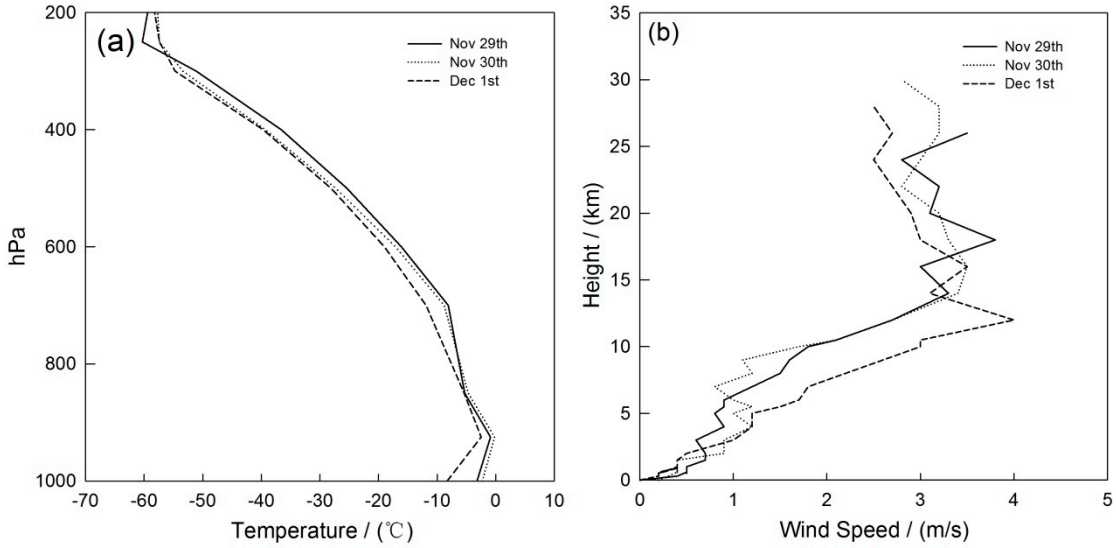

4. Conclusions

In this study, the long-term visibility, PM mass concentration and mixing layer height were investigated from 2009-2012 in the multi-cities of central Liaoning over Northeast China to represent the horizontal and vertical meteorological elements on air pollution in these economically developed urban-industry areas.

(1) The lower annual mean visibility in the multi-cities of central Liaoning suggests the poor atmospheric quality in Northeast China. The pollution load (PM×MLH) shown the higher PM concentration in the near-surface with a weaker vertical diffusion in Anshan. The highest pollution load (PM × MLH) in Shenyang may due to the contribution of pollutants transportation and the local emission sources.

(2) The monthly variation of MLH may be related to the seasonal radiation flux during the year to affect visibility by vertical pollutants diffusion. The increased fine particle concentration from September to November and even to the January in the next year was partially attributed to the biomass burning emissions and heating sources under lower MLH in winter.

(3) The better relationship between wind speed and MLH shown the vertical transportation of air pollutant to get better visibility.

(4) The MLH on the non haze-fog days was about 1.2 and 1.5 times higher than that on hazy and fog days. These noted that the MLH during fog events have shown more declining trend than haze event which indicate the relatively large impact of dynamic effects on the fog pollution in the multi-cities of central Liaoning.

However, further studies are still needed to taking into account the more boundary layer data and their impacts air pollution in the Northeast China.

Acknowledgments: This work is financially supported by grants from the Project (41375153) and (41605112) supported by NSFC, the National Key Project of Basic Research (2014CB441201), the CAMS Basis Research Project (2014R17), the Climate Change Special Fund of CMA (CCSF201504) and the Special Project of Doctoral Research supported by Liaoning Provincial Meteorological Bureau (D201501).

Author Contributions: Hujia Zhao wrote the article; Huizheng Che designed the experiments; Hujia Zhao, and Huizheng Che, performed the experiments; Hongbin Yang, and Yuche Liu calculated the mixing layer data; Yanjun Ma, and Yangfeng Wang analyzed the data; Yaqiang Wang, Hong Wang and Xiaoye Zhang helped perform the statistical analysis.

Conflicts of Interest: The authors declare no conflict of interest

References

1. Sloane, C.S. Meteorological adjusted air quality trends: visibility. *Atmos. Environ.* **1984**, *18*, 1217–1229.
2. Schichtel, B.A.; Husar, R.B.; Falke, S.R.; Wilson, W.E. Haze trends over the United States, 1980–1995. *Atmos. Environ.* **2001**, *35*, 5205–5210.
3. Watson, J.G. Visibility: Science and Regulation. *J.Air Waste Manage. Assoc.* **2002**, *52*, 628–713.
4. Molnár, A.; Mészáros, E.; Imre, K.; Rüll, A. Trends in visibility over Hungary between 1996 and 2002. *Atmos. Environ.* **2008**, *42*, 2621–2629.
5. Chan, Y.C.; Simpson, R.W.; Mctainsh, G.H.; Vowles, P.D.; Cohen, D.D.; Bailey, G.M. Source apportionment of visibility degradation problems in Brisbane (Australia) using the multiple linear regression techniques. *Atmos. Environ.* **1999**, *33*, 3237–3250.
6. Sloane, C.S.; Watson, J.; Chow, J.; Pritchett, L.; Willard, R.L. Size–segregated fine particle measurements by chemical species and their impact on visibility impairment in Denver. *Atmos. Environ.* Part A. General Topics. **1991**, *25*, 1013–1024.
7. Kim, Y.J.; Kim, K.W.; Kim, S.D.; Lee, B.K.; Han, J.S. Fine Particulate Matter Characteristics and Its Impact on Visibility Impairment at Two Urban Sites in Korea: Seoul and Incheon. *Atmos. Environ.* **2006**, *40*, S593–S605.
8. Elias, T.; Haeffelin, M.; Drobinski, P.; Gomes, L.; Rangognio, J.; Bergot, T.; Chazette, P.; Raut, J.C.; Colomb, M. Particulate Contribution to Extinction of Visible Radiation: Pollution, Haze and Fog. *Atmos. Res.* **2009**, *92*, 443–454.
9. Ghim, Y.S.; Moon, K.C.; Lee, S.Y.; Kim, Y.P. Visibility trends in Korea during the past two decades. *J. Air Waste Manage. Assoc.* **2005**, *55*, 73–82.
10. Pope, C.R., Burnett, R., M.J., T., Calle, E., Krewski, D., Ito, K., Thurston, G. Lungcancer, cardiopulmonary mortality, and long-term exposure to fine particulate air pollution. *JAMA.* **2002**, *287*, 1132–1141.
11. Tsai, Y.I. Atmospheric visibility trends in an urban area in Taiwan1961–2003. *Atmos. Environ.* **2005**, *39*, 5555–5567.
12. Wilson, W.E.; Suh, H.H. Fine particles and coarse particles: concentration relationships relevant to epidemiological studies. *J. Air Waste Manage. Assoc.* **1997**, *47*, 1238–1249.
13. Husar, R.B.; Holloway, J.M.; Patterson, D.E.; Wilson, W.E. Spatial and temporal pattern of eastern US haziness: a summary. *Atmos. Environ.* **1981**, *15*, 1919–1928.
14. Gurjar, B.R.; Lelieveld, J. New directions: megacities and global change. *Atmos. Environ.* **2005**, *39*, 391–393.
15. Tsai, Y.I.; Kuo, S.C.; Lee, W.J.; Chen, C.L.; Chen, P.T. Long-term visibility trends in one highly urbanized, one highly industrialized and two rural areas of Taiwan. *Sci. Total Environ.* **2007**, *382*, 324–341.
16. Lawrence, M.G.; Butler, T.M.; Steinkamp, J.; Gurjar, B.R.; Lelieveld, J. Regional pollution potentials of megacities and other major population centers. *Atmos. Chem. Phys.* **2007**, *7*, 3969–3987.
17. Doyle, M.; Dorling, S. Visibility trends in the UK 1950–1997. *Atmos. Environ.* **2002**, *36*, 3161–3172.
18. Mahowald, N.M.; Ballantine, J.A.; Feddema, J.; Ramankutty, N. Global trends in visibility: implications for dust sources. *Atmos. Chem. Phys.* **2007**, *7*, 3309–3339.
19. Aron, R. Mixing height – an inconsistent indicator of potential air pollution concentrations. *Atmos. Environ.* **1983**, *17*, 2193–2197.
20. Stull, R. B. An Introduction to Boundary Layer Meteorology. Kluwer Academic Publishers, Dordrecht, **1988**.
21. Stull, S. An Introduction to Boundary Layer Meteorology. Kluwer Academic Publishers. **1991**.
22. Subrahamanyam, D.B.; Ramchandran, R.; Sen G. K.; Mandal, T.K. Variability of mixed layer heights over the Indian Ocean and central Arabian Sea during INDOEX, IFP-99. *Bound.-Layer Meteorol.* **2003**, *107*, 683–695.

23. Alappattu, D.P.; Kunhikrishnan, P.K.; Aloysius, M.; Mohan, M. A case study of atmospheric boundary layer features during winter over a tropical inland station — Kharagpur (22.32°N, 87.32°E). *J. Earth Syst. Sci.* **2009**, *118*, 281–293. http://dx.doi.org/10.1007/s12040-009-0028-3.
24. Kompalli S.K.; Babu S.S.; Moorthy K.K.; Manoj, M. R.; Kumar, N. K.; Shaeb, K.H. B.; Joshi, A. K. Aerosol black carbon characteristics over Central India: Temporal variation and its dependence on mixed layer height. *Atmos. Res.* **2014**, *147*, 27-37.
25. Oleniacz, R.; Bogacki, M.; Szulecka, A.; Rzeszutek, M.; Mazur, M. Assessing the impact of wind speed and mixing-layer height on air quality in Krakow (Poland) in the years 2014-2015. *JCEEA.* **2016**, s, *315–342*.
26. Yang, H.; Liu, W.; Lu, Y.; Xie, P.; Xu, L.; Zhao, X.; Yu, T.; Yu, J. PBL observations by lidar at Peking. *Optical Tech.* **2005**, *31*, 221–226.
27. Quan, J.; Gao, Y.; Zhang, Q.; Tie, X.; Cao, J.; Han, S.; Meng, J.; Chen, P.; Zhao, D. Evolution of Planetary Boundary Layer under Different Weather Conditions, and Its Impact on Aerosol Concentrations. *Particuology.* **2013**, *11*, 34–40.
28. Zhang, Q.; Quan, J.; Tie, X.; Li, X.; Liu, Q.; Gao, Y.; Zhao, D. Effects of meteorology and secondary particle formation on visibility during heavy haze events in Beijing, China. *Sci. Total Environ.* **2105**, *502*, 578–584. doi:10.1016/j.scitotenv.2014.09.079.
29. Tang, G.; Zhu, X.; Hu, B.; Xin, J.; Wang, L.; Münkel, C.; Mao, G.; Wang, Y. Impact of emission controls on air quality in Beijing during APEC 2014: lidar ceilometer observations. *Atmos. Chem. Phys.* **2015**, *15*, 12667–12680. doi:10.5194/acp-15-12667-2015.
30. Tang, G.; Zhang, J.; Zhu, X.; Song, T.; Münkel, C.; Hu, B.; Schäfer, K.; Liu, Z.; Zhang, J.; Wang, L.; Xin, J.; Suppan, P.; Wang, Y. Mixing layer height and its implications for air pollution over Beijing, China. *Atmos. Chem. Phys.* **2016**, *16*, 2459–2475. doi:10.5194/acp-16-2459-2016.
31. Chang, D.; Song, Y.; Liu, B. Visibility trends in six megacities in China 1973–2007. *Atmos. Res.* **2009**, *94*, 161–167.
32. Che, H.Z.; Zhang, X.Y.; Li, Y.; Zhou, Z.J.; Qu, J.J.; Hao, X.J. Haze trends over the capital cities of 31 provinces in China, 1981–2005. *Theor. Appl. Climatol.* **2009**, *97*, 235–242.
33. Ji, C.Y.; Lin, P.; Li, X.; Liu, Q.; Sun, D.; Wang, S. Monitoring urban expansion with remote sensing in China. *Int. J. Remote Sens.* **2001**, *22*, 1441–1455.
34. Weng, Q. Land use change analysis in the Zhujiang Delta of China using satellite remote sensing, GIS and stochastic modeling. *J. Environ. Manage.* **2002**, *64*, 273–284.
35. Zhang, Q.; Streets, D.G.; Carmichael, G.R.; He, K.B.; Huo, H.; Kannari, A.; Klimont, Z.; Park, I.S.; Reddy, S.; Fu, J.S.; Chen, D.; Duan, L.; Lei, Y.; Wang, L.T.; Yao, Z.L. Asian emissions in 2006 for the NASAINTEX–B mission. *Atmos. Chem. Phys.* **2009**, *9*, 5131–5153.
36. Zhang, R.; Jing, J.; Tao, J.; Hsu, S.C.; Wang, G.; Cao, J.; Lee, C.S.L.; Zhu, L.; Chen, Z.; Zhao, Y.; Shen, Z. Chemical characterization and source apportionment of PM2.5 in Beijing: seasonal perspective. *Atmos. Chem. Phys.* **2013**, *13*, 7053–7074.
37. Chan, C.K.; Yao, X. Air pollution in megacities in China. *Atmos. Environ.* **2008**, *42*, 1–42.
38. Tie, X.X.; Cao, J.J. Aerosol pollution in China: present and future impact on environment. *Particuology* **2009**, *7*, 426–431.
39. Yao, L.; Lu, N.; Yue, X.F.; Du, J.; Yang, C.D. Comparison of hourly PM2.5 observations between urban and suburban areas in Beijing, China. *Int. J. Environ. Res. Public Health* **2015**, *12*, 12264–12276.
40. Zhang, T.H.; Liu, G.; Zhu, Z.M.; Gong, W.; Ji, Y.X.; Huang, Y.S. Real-time estimation of satellite-derived $PM_{2.5}$ based on a semi-physical geographically weighted regression model. *Int. J. Environ. Res. Public Health* **2016**, *13*, 974.
41. Li, Y.; Tao, J.; Zhang, L.M.; Jia, X.F.; Wu, Y.F. High Contributions of Secondary Inorganic Aerosols to PM2.5 under Polluted Levels at a Regional Station in Northern China. *Int. J. Environ. Res. Public Health* **2016**, *13*, 1202.
42. Sun, Y.; Zhou, X.; Wai, K.; Yuan, Q.; Xu, Z.; Zhou, S.; Qi, Q.; Wang, W. Simultaneous Measurement of Particulate and Gaseous Pollutants in an Urban City in North China Plain during the Heating Period: Implication of Source Contribution. *Atmos. Res.* **2013**, *134*, 24–34.

43. Deng, J.J.; Wang, T.J.; Jiang, Z.Q.; Min, X.; Zhang, R.; Huang, X.; Zhu, J. Characterization of Visibility and Its Affecting Factors over Nanjing, China. *Atmos. Res.* **2011**, *101*, 681–691.
44. Yang, F.; Chen, H.; Du, J.; Yang, X.; Gao, S.; Chen, J.; Geng, F. Evolution of the Mixing State of Fine Aerosols during Haze Events in Shanghai. *Atmos. Res.* **2012**, *104–105*, 193–201.
45. Cheng, Z.; Wang, S.X.; Jiang, J.K.; Fu, Q.; Chen, C.; Xu,B.; Yu, J.; Fu, X.; Hao, J. Long-term Trend of Haze Pollution and Impact of Particulate Matter in the Yangtze River Delta, China. *Environ. Pollut.* **2013**, *182*, 101–110.
46. Yue, D.; Hu, M.; Wu, Z.; Guo, S.; Wen, M.; Nowak, A.; Wehner, B.; Wiedensohler, A.; Takegawa, N.; Kondo, Y.; Wang, X.; Li, Y.; Zeng, L.; Zhang, Y. Variation of Particle Number Size Distributions and Chemical Compositions at the Urban and Downwind Regional Sites in the Pearl River Delta during Summertime Pollution Episodes. *Atmos. Chem. Phys.* **2010**, *10*, 9431–9439.
47. Zhang, X.; Wang, Y.; Niu, T.; Zhang, X.; Gong, S.; Zhang, Y.; Sun, J. Atmospheric Aerosol Compositions in China: Spatial/Temporal Variability, Chemical Signature, Regional Haze Distribution and Comparisons with Global Aerosols. *Atmos. Chem. Phys.* **2012**, *12*, 779–799.
48. Zhang, Y.H.; Zhu, X.L.; Slanina, S.; Shao, M.; Zeng, L.M.; Hu, M.; Bergin, M.; Salmon, S. Aerosol pollution in some Chinese cities. *Pure Appl. Chem.* **2004**, *76*, 1227–1239.
49. Che, H.Z.; Zhang, X.Y.; Li, Y.; Zhou, Z.J.; Qu, J.J. Horizontal visibility trends in China 1981–2005. *Geophys. Res. Lett.* **2007**, *34*, L24706–L24710.
50. Hu, X.; Ma, Z.; Lin, W.; Zhang, H.; Hu, J.; Wang, Y.; Xu, X.; Fuentes, J. D.; Xue, M. Impact of the Loess Plateau on the atmospheric boundary layer structure and air quality in the North China Plain: a case study. *Sci. Total Environ.* **2014**, *499*, 228–237. doi:10.1016/j.scitotenv.2014.08.053.
51. Wang, S.; Hao, J. Air Quality Management in China: Issues, Challenges, and Options. *J. Environ. Sci.-China.* **2012**, *24*: 2–13.
52. Zhao, H.; Che, H.; Zhang, X.; Ma, Y.; Wang, Y.; Wang, H.; Wang, Y. Characteristics of Visibility and Particulate Matter (PM) in an Urban Area of Northeast China. *Atmos. Pollut. Res.* **2013**, *4*, 427–434.
53. Zhao, H.; Che, H.; Ma, Y.; Xia, X.; Wang, Y.; Wang, P.; Wu, X. Temporal variability of the visibility, particulate matter mass concentration and aerosol optical properties over an urban site in Northeast China. *Atmos. Res.* **2015**, *166*, 204–212.
54. Li, Y.; Zhao, H.; Wu, Y. Characteristics of Particulate Matter during Haze and Fog (Pollution) Episodes over Northeast China, Autumn 2013. *Aerosol Air Qual. Res.* **2015**, *15*, 853–864.
55. GB/T13201, Technical guidelines for environmental impact assessment General principle, Appendix B, **1993**, China.
56. He, G.X.; Yu, C.W.F.; Lu, C.; Deng, Q.H. The influence of synoptic pattern and atmosphere boundary layer on PM10 and urban heat island. *Indoor. Built. Environ.* **2013**, *22*, 796–807.
57. Li, M.; Tang, G.Q.; Huang, J.; Liu, Z.R.; An, J.L.; Wang, Y.S. Characteristics of winter atmospheric mixing layer height in Beijing-Tianjin-Hebei region and their relationship with the atmospheric pollution. *Environ. Sci.* **2015**, *36*, 1935-1943.(in Chinese)
58. Hennigan, C.J.; Bergin, M.H.; Dibb, J.E.; Weber, R.J. Enhanced Secondary Organic Aerosol Formation Due to Water Uptake by Fine Particles. *Geophys. Res. Lett.* **2008**, *35*, 102. doi: 10.1029/2008GL035046.
59. Kamp, D.; McKendry, I. Diurnal and seasonal trends in convective mixed-layer heights estimated from two years of continuous ceilometer observations in Vancouver, BC. *Bound.-Lay. Meteorol.* **2010**, *137*, 459–475.
60. Muňoz, R. C.; Undurraga, A. A. Daytime mixed layer over the Santiago Basin: Description of two years of observations with a lidar ceilometer. *J. Appl. Meteorol. Clim.* **2010**, *49*, 1728–1741.
61. Sun, Y. L. Physicochemical characterizations of airborne particulate matter in the typical regions of China and its impact on regional environment. *Doctoral thesis,* Beijing Normal University, China, **2005**.

62. Xu, J.; Bergin, M.H.; Yu, X.; Liu, G.; Zhao, J.; Carrico, C.M.; Baumann, K. Measurement of aerosol chemical, physical and radiative properties in the Yangtze delta region of China. *Atmos. Environ.* **2002**, *36*, 161–173.
63. Duan, F.K.; Liu, X.D.; Yu, T.; Cachier, H. Identification and estimate of biomass burning contribution to the urban aerosol organic carbon concentrations in Beijing. *Atmos. Environ.* **2004**, *38*, 1275–1282.
64. Zheng, X.Y.; Liu, X.D.; Zhao, F.H.; Duan, F.K.; Yu, T.; Cachier, H. Seasonal characteristics of biomass burning contribution to Beijing aerosol. *Sci. China, Ser. B Chem. Life Sci. Earth Sci.* **2005**, *48*, 481–488.
65. Sun, Y. L.; Zhuang, G. S.; Wang, Y.; Han, L. H.; Guo, J.H.; Dan, M.; Zhang, W.J.; Wang, Z.F.; Hao, Z.P. The air-borne particulate pollution in Beijing concentration, composition, distribution and sources. *Atmos. Environ.* **2004**, *38*, 5991–6004.
66. Guinot, B.; Cachier, H.; Sciare, J.; Tong, Y.; Wang, X.; Yu, J. Beijing aerosol: atmospheric interactions and new trends. *J. Geophys. Res.* **2007**, *112*, 928–935. D14314. doi:10.1029/2006JD008195.
67. Cao J J, Lee S C, Chow J C, Watson J G, Ho K F, Zhang R J et al. Spatial and seasonal distributions of carbonaceous aerosols over China. *J. Geophys. Res.* **2007**, *D112*, 22–11. D22S11. DOI: 10.1029/2006JD008205.
68. Cao, J.J.; Zhu, C.S.; Chow, J.C.; Watson, J.G.; Han, Y.M.; Wang, G.H.; Shen, Z.X.; An, Z.S. Black carbon relationships with emissions and meteorology in Xi'an China. *Atmos. Res.* **2009**, *94*, 194–202.
69. Gomez, B.; Smith, C.G. Visibility at Oxford 1926–1985. *Weather*. **1987**, *39*, 379–384.
70. Du, H.; Kong, L.; Cheng, T.; Chen, J.; Du, J.; Li, L.; Xia, X.; Leng, C.; Hang, G. Insights into Summertime Haze Pollution Events over Shanghai Based on Online Water-soluble Ionic Composition of Aerosols. *Atmos. Environ*. **2011**, *45*, 5131–5137.
71. Shi, Y.; Chen, J.M.; Hu, D.W.; Wang, L.; Yang, X.; Wang, X.M. Airborne submicron particulate (PM_1) pollution in Shanghai, China: Chemical variability, formation/dissociation of associated semi-volatile components and the impacts on visibility. *Sci. total. Environ.* **2014**, *473–474*, 199–206.